Complex critical points and curved geometries in Lorentzian EPRL spinfoam amplitude

Dongxue Qu

Florida Atlantic University

Collaborators: Muxin Han, Zichang Huang and Hongguang Liu

Oct. 5th, 2021@ILQGS

Outline

1. Motivation and Results
2. EPRL Spinfoam Model
3. Real and Complex critical points
4. Numerical Implementation: Δ_3
5. Numerical Implementation: 1-5 Pachner Move

Outline

Motivation and Results

- The semiclassical consistency is an important requirement in LQG.
- We focus on 4-dimensional Lorentzian EPRL spinfoam formulation.

Motivation and Results

- The semiclassical consistency is an important requirement in LQG.
- We focus on 4-dimensional Lorentzian EPRL spinfoam formulation.
- Semiclassical approximation $\Longrightarrow$ Large-j asymptotics of spinfoam amplitude.
  [Asante, Bahr, Barrett, Bianchi, Bonzom, Conrady, Ding, Dittrich, Dona, Engle, Freidel, Gozzini, Haggard, Han, Hellmann, Huang, Kaminski, Kisielowski, Liu, Livine, Magliaro, Perini, Pereira, Riello, Rovelli, Sahlmann, Sarno, Speziale, Zhang, etc.]
- Asymtotics of the spinfoam amplitude relates to Regge calculus

Motivation and Results

- The semiclassical consistency is an important requirement in LQG.
- We focus on 4-dimensional Lorentzian EPRL spinfoam formulation.
- Semiclassical approximation $\Longrightarrow$ Large-j asymptotics of spinfoam amplitude.
  [Asante, Bahr, Barrett, Bianchi, Bonzom, Conrady, Ding, Dittrich, Dona, Engle, Freidel, Gozzini, Haggard, Han, Hellmann, Huang, Kaminski, Kisielowski, Liu, Livine, Magliaro, Perini, Pereira, Riello, Rovelli, Sahlmann, Sarno, Speziale, Zhang, etc.]
- Asymtotics of the spinfoam amplitude relates to Regge calculus
- Recent progress in numerics on spinfoam models
  - sl2cfoam based on $15j$ + boosters [Dona, Fanizza, Sarno, Speziale, Gozzini 2018-2021]
  - Spinfoam renormalization [Bahr, Dittrich, Steinhaus, 2016-2021]
  - Effective spinfoam model [Asante, Dittrich, Haggard, 2020-2021]
  - Asymptotics expansion, Lefschetz thimble, Monte-Carlo [Han, Huang, Liu, DQ, 2020-2021]

Motivation and Results

- The semiclassical consistency is an important requirement in LQG.
- We focus on 4-dimensional Lorentzian EPRL spinfoam formulation.
- Semiclassical approximation $\Longrightarrow$ Large-j asymptotics of spinfoam amplitude.
  [Asante, Bahr, Barrett, Bianchi, Bonzom, Conrady, Ding, Dittrich, Dona, Engle, Freidel, Gozzini, Haggard, Han, Hellmann, Huang, Kaminski, Kisielowski, Liu, Livine, Magliaro, Perini, Pereira, Riello, Rovelli, Sahlmann, Sarno, Speziale, Zhang, etc.]
- Asymtotics of the spinfoam amplitude relates to Regge calculus
- Recent progress in numerics on spinfoam models
  - sl2cfoam based on $15j$ + boosters [Dona, Fanizza, Sarno, Speziale, Gozzini 2018-2021]
  - Spinfoam renormalization [Bahr, Dittrich, Steinhaus, 2016-2021]
  - Effective spinfoam model [Asante, Dittrich, Haggard, 2020-2021]
  - Asymptotics expansion, Lefschetz thimble, Monte-Carlo [Han, Huang, Liu, DQ, 2020-2021]
- Simplicial complex, sum over j $\to$ Flatness problem:

The EPRL spinfoam amplitude seems to be dominated *only* by flat Regge geometries in the semiclassical regime.

The numerics demonstrates curved geometries whose contributions are not small in EPRL spinfoam amplitudes.

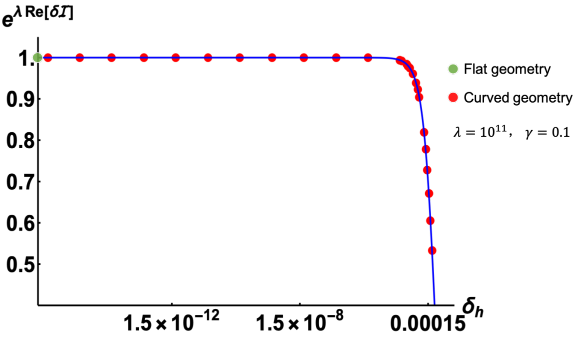

Horizontal axis: deficit angle δ_h; Vertical axis: $\propto$ Amplitudes

In spinfoam, large spin parameter λ is a *finite* expansion parameter.

For any large but finite λ, there exists relatively small deficit angles such that the amplitude is not small.

$\gamma = 0.1$

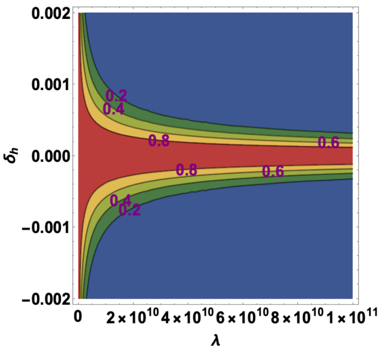

$\lambda = 5 \times 10^{10}$

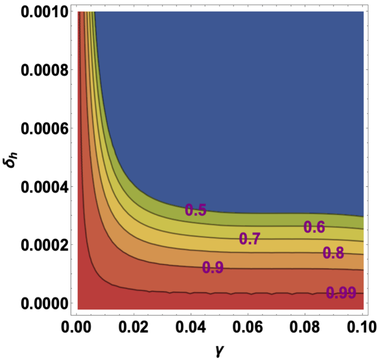

The non-blue regime of curved geometries where the amplitude is not small.

Effective action: Regge action plus "high curvature correction"

$$\mathcal{S} = i\mathcal{I}_R[\mathbf{g}(r)] + a_2\delta_h^2 + a_3\delta_h^3 + a_4\delta_h^4 + O(\delta_h^5),$$

- These curved geometries come from complex critical points.
- A warm-up example

$$A_\lambda(r) = \int_{-\infty}^{+\infty} e^{\lambda\left[ix^2 - r(x+1)^2\right]} dx, \quad r \geq 0, \quad \lambda \gg 1$$

The critical point: $x_c = \frac{r}{r-i} \begin{cases} r = 0 & \text{real critical point} \\ r \neq 0 & \text{complex critical point} \end{cases},$

$$A_\lambda(r) = \frac{\sqrt{\pi}}{\sqrt{\lambda(r-i)}} e^{\lambda\left[ix_c^2 - r(x_c+1)^2\right]},$$

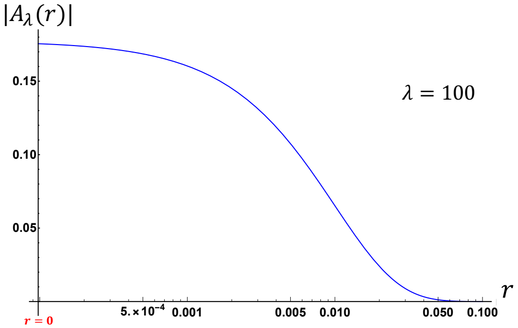

Similar ideas appeared in

[Asante, Dittrich, Haggard, 2020]

[Han, 2013]

[Engle, Kaminski, Oliveira 2020]

Motivation and Results

- Δ_3: relaxing cosine problem.
- 1-5 Pachner move: reduce the spinfoam amplitude to integral over Regge geometries:

$$\left(\frac{1}{\lambda}\right)^{\frac{N}{2}} \int \prod_{m=1}^{5} \mathrm{d}l_{m6}\, e^{\lambda \mathcal{S}(r, Z(r))} \mathscr{N}_r \left[1 + O(1/\lambda)\right],$$

Effective action $\mathcal{S}$ is Regge action plus “high curvature correction”.

Outline

EPRL Spinfoam Model

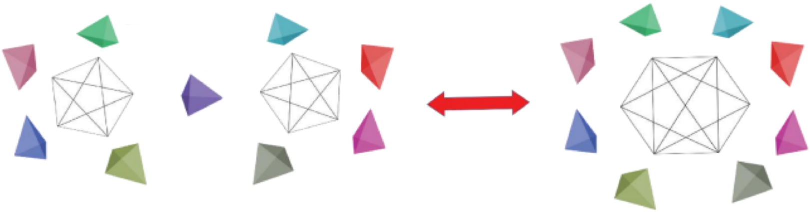

4-d triangulation $\mathcal{K}$

- 4-simplices: σ
- tetrahedra: τ
- triangles: t

dual complex $\mathcal{K}^*$

- vertices: v
- oriented edges: e
- oriented faces: f : h (internal), b (boundary)

A spinfoam assigns an SU(2) spin j_f to each face f: j_h, j_b.

EPRL Spinfoam Amplitude

The spinfoam amplitude in the integral representation:

$$A(\mathcal{K}) \quad = \quad \sum_{\{j_h\}} \prod_h d_{j_h} \int [\mathrm{d}g\mathrm{d}\mathbf{z}]\, e^{S\left(j_h, g_{ve}, \mathbf{z}_{vf}; j_b, \xi_{eb}\right)},$$
$$[\mathrm{d}g\mathrm{d}\mathbf{z}] = \prod_{(v,e)} \mathrm{d}g_{ve} \prod_{(v,f)} \mathrm{d}\Omega_{\mathbf{z}_{vf}},$$

- $|j_b, \xi_{eb}\rangle$: SU(2) boundary coherent state.
- $\mathbf{z}_{vf} \in \mathbb{CP}^1$.
- $g_{ve} \in \mathrm{SL}(2, \mathbb{C})$.
- phase amplitude $d_{j_h} = 2j_h + 1$.
- dg_{ve} is the Haar measure, $\mathrm{d}\Omega_{\mathbf{z}_{vf}}$ is a scaling invariant measure on $\mathbb{CP}^1$.

EPRL spinfoam action

The spinfoam action S is given by

$$
\begin{aligned}
S &= \sum_{(e',x)} j_h F_{(e',x)} + \sum_{(e,b)} j_b F_{(e,b)} + \sum_{(e',b)} j_b F_{(e',b)}, \\
F_{(e,b)} &= 2\ln \frac{\langle Z_{veb}, \xi_{eb} \rangle}{\| Z_{veb} \|} + i\gamma \ln \| Z_{veb} \|^2 , \quad Z_{vef} = g_{ve}^{\dagger} \mathbf{z}_{vf} \\
\text{or} & \quad 2\ln \frac{\langle \xi_{eb}, Z_{v'eb} \rangle}{\| Z_{v'eb} \|} - i\gamma \ln \| Z_{v'eb} \|^2 , \\
F_{(e',f)} &= 2\ln \frac{\langle Z_{ve'f}, Z_{v'e'f} \rangle}{\| Z_{ve'f} \| \, \| Z_{v'e'f} \|} + i\gamma \ln \frac{\| Z_{ve'f} \|^2}{\| Z_{v'e'f} \|^2},
\end{aligned}
$$

EPRL spinfoam action

The spinfoam action S is given by

$$
\begin{aligned}
S &= \sum_{(e',x)} j_h F_{(e',x)} + \sum_{(e,b)} j_b F_{(e,b)} + \sum_{(e',b)} j_b F_{(e',b)}, \\
F_{(e,b)} &= 2\ln \frac{\langle Z_{veb}, \xi_{eb}\rangle}{\|Z_{veb}\|} + i\gamma \ln \|Z_{veb}\|^2, \quad Z_{vef} = g_{ve}^{\dagger} \mathbf{z}_{vf} \\
\text{or} \quad & 2\ln \frac{\langle \xi_{eb}, Z_{v'eb}\rangle}{\|Z_{v'eb}\|} - i\gamma \ln \|Z_{v'eb}\|^2, \\
F_{(e',f)} &= 2\ln \frac{\langle Z_{ve'f}, Z_{v'e'f}\rangle}{\|Z_{ve'f}\| \, \|Z_{v'e'f}\|} + i\gamma \ln \frac{\|Z_{ve'f}\|^2}{\|Z_{v'e'f}\|^2},
\end{aligned}
$$

Continuous gauge freedom and gauge fixing:

- For each $\mathbf{z}_{vf}$, $\mathbf{z}_{vf} \mapsto \lambda_{vf}\mathbf{z}_{vf}$, $\lambda_{vf} \in \mathbb{C} \Longrightarrow \mathbf{z}_{vf} = (1, \alpha_{vf})^T$.

EPRL spinfoam action

The spinfoam action S is given by

$$
\begin{aligned}
S &= \sum_{(e',x)} j_h F_{(e',x)} + \sum_{(e,b)} j_b F_{(e,b)} + \sum_{(e',b)} j_b F_{(e',b)}, \\
F_{(e,b)} &= 2\ln \frac{\langle Z_{veb}, \xi_{eb}\rangle}{\|Z_{veb}\|} + i\gamma \ln \|Z_{veb}\|^2, \quad Z_{vef} = g_{ve}^\dagger \mathbf{z}_{vf} \\
\text{or} \quad & 2\ln \frac{\langle \xi_{eb}, Z_{v'eb}\rangle}{\|Z_{v'eb}\|} - i\gamma \ln \|Z_{v'eb}\|^2, \\
F_{(e',f)} &= 2\ln \frac{\langle Z_{ve'f}, Z_{v'e'f}\rangle}{\|Z_{ve'f}\|\,\|Z_{v'e'f}\|} + i\gamma \ln \frac{\|Z_{ve'f}\|^2}{\|Z_{v'e'f}\|^2},
\end{aligned}
$$

Continuous gauge freedom and gauge fixing:

- For each $\mathbf{z}_{vf}$, $\mathbf{z}_{vf} \mapsto \lambda_{vf}\mathbf{z}_{vf}$, $\lambda_{vf} \in \mathbb{C} \Longrightarrow \mathbf{z}_{vf} = (1, \alpha_{vf})^T$.
- At each v, $g_{ve} \mapsto x_v^{-1} g_{ve}$, $\mathbf{z}_{vf} \mapsto x_v^\dagger \mathbf{z}_{vf}$, $x_v \in \mathrm{SL}(2,\mathbb{C}) \Longrightarrow$ one $g_{ve} = 1$

EPRL spinfoam action

The spinfoam action S is given by

$$
\begin{aligned}
S &= \sum_{(e',x)} j_h F_{(e',x)} + \sum_{(e,b)} j_b F_{(e,b)} + \sum_{(e',b)} j_b F_{(e',b)}, \\
F_{(e,b)} &= 2\ln \frac{\langle Z_{veb}, \xi_{eb}\rangle}{\|Z_{veb}\|} + i\gamma \ln \|Z_{veb}\|^2 , \quad Z_{vef} = g_{ve}^{\dagger} \mathbf{z}_{vf} \\
\text{or} \quad & 2\ln \frac{\langle \xi_{eb}, Z_{v'eb}\rangle}{\|Z_{v'eb}\|} - i\gamma \ln \|Z_{v'eb}\|^2 , \\
F_{(e',f)} &= 2\ln \frac{\langle Z_{ve'f}, Z_{v'e'f}\rangle}{\|Z_{ve'f}\| \, \|Z_{v'e'f}\|} + i\gamma \ln \frac{\|Z_{ve'f}\|^2}{\|Z_{v'e'f}\|^2},
\end{aligned}
$$

Continuous gauge freedom and gauge fixing:

- For each $\mathbf{z}_{vf}$, $\mathbf{z}_{vf} \mapsto \lambda_{vf}\mathbf{z}_{vf}$, $\lambda_{vf} \in \mathbb{C} \Longrightarrow \mathbf{z}_{vf} = (1, \alpha_{vf})^T$.
- At each v, $g_{ve} \mapsto x_v^{-1} g_{ve}$, $\mathbf{z}_{vf} \mapsto x_v^{\dagger}\mathbf{z}_{vf}$, $x_v \in \mathrm{SL}(2,\mathbb{C}) \Longrightarrow$ one $g_{ve} = 1$
- At each e, $g_{v'e} \mapsto g_{v'e}h_e^{-1}$, $g_{ve} \mapsto g_{ve}h_e^{-1}$, $h_e \in \mathrm{SU}(2) \Longrightarrow g_{v'e}$ to be upper-triangular matrix.

  (any $g \in \mathrm{SL}(2,\mathbb{C})$ can be written as $g = kh$ where k is upper-triangular and $h \in \mathrm{SU}(2)$).

Real parametrization:

$$\begin{aligned} g_{v'e} &= \mathring{g}_{v'e} \begin{pmatrix} 1 + \frac{x^1_{v'e}}{\sqrt{2}} & \frac{x^2_{v'e}+iy^2_{v'e}}{\sqrt{2}} \\ 0 & \mu_{v'e} \end{pmatrix} \in \mathrm{SL}(2,\mathbb{C}), \\ g_{ve} &= \mathring{g}_{ve} \begin{pmatrix} 1 + \frac{x^1_{ve}+iy^1_{ve}}{\sqrt{2}} & \frac{x^2_{ve}+iy^2_{ve}}{\sqrt{2}} \\ \frac{x^3_{ve}+iy^3_{ve}}{\sqrt{2}} & \mu_{ve} \end{pmatrix} \in \mathrm{SL}(2,\mathbb{C}) \\ \mathbf{z}_{vf} &= (1, \mathring{\alpha}_{vf} + x_{vf} + iy_{vf}) \in \mathbb{CP}^1. \end{aligned}$$

- $x_{ve}, y_{ve}, x_{vf}, y_{vf}$ are real numbers.
- $\mathring{g} \in \mathrm{SL}(2,\mathbb{C})$ and $\mathring{\alpha} \in \mathbb{C}$ will be a critical point of S.

Therefore,

$$S\left(j_h, g_{ve}, \mathbf{z}_{vf}\right) = S(j_h, x_{ve}, y_{ve}, x_{vf}, y_{vf})$$

will be analytic continued (locally) to the holomorphic function

$$\mathcal{S}(j_h, x_{ve}, y_{ve}, x_{vf}, y_{vf}), \quad j_h, x_{ve}, y_{ve}, x_{vf}, y_{vf} \in \mathbb{C}$$

EPRL Spinfoam Amplitude

LQG area spectrum: $\mathfrak{a} = 8\pi\gamma\ell_p^2\sqrt{j(j+1)}, \quad \mathfrak{a} \gg \ell_p^2 \Longleftrightarrow j \gg 1$

Semiclassical regime $\Longleftrightarrow$ large-j regime.

EPRL Spinfoam Amplitude

LQG area spectrum: $\mathfrak{a} = 8\pi\gamma\ell_p^2\sqrt{j(j+1)}, \quad \mathfrak{a} \gg \ell_p^2 \Longleftrightarrow j \gg 1$

Semiclassical regime $\Longleftrightarrow$ large-j regime.

To probe the semiclassical regime, we scale both boundary and internal spins

$$j_b \to \lambda j_b, \quad j_h \to \lambda j_h, \quad \lambda \gg 1$$

EPRL Spinfoam Amplitude

LQG area spectrum: $\mathfrak{a} = 8\pi\gamma\ell_p^2\sqrt{j(j+1)}, \quad \mathfrak{a} \gg \ell_p^2 \Longleftrightarrow j \gg 1$

Semiclassical regime $\Longleftrightarrow$ large-j regime.

To probe the semiclassical regime, we scale both boundary and internal spins

$$j_b \to \lambda j_b, \quad j_h \to \lambda j_h, \quad \lambda \gg 1$$

Apply the Poisson summation to the EPRL spinfoam amplitude:

$$\begin{aligned} A(\mathcal{K}) &= \sum_{\{k_h \in \mathbb{Z}\}} \int_{\mathbb{R}} \prod_h \mathrm{d}j_h \prod_h 2\lambda\, d_{\lambda j_h} \int [\mathrm{d}g\mathrm{d}\mathbf{z}]\, e^{\lambda S^{(k)}}, \\ S^{(k)} &= S + 4\pi i \sum_h j_h k_h, \end{aligned}$$

j_h is continuous.

Outline

Real Critical Points

- The integral in the spinfoam amplitude has the following form:

$$\int \mathrm{d}^N x \, \mu(x) \, e^{\lambda S(r,x)}, \quad \lambda \gg 1,$$

where r is boundary data, x is integration variable.

$$r = (j_b, \xi_{eb}), \quad x = \{j_h, x_{ve}, y_{ve}, x_{vf}, y_{vf}\} \in \mathbb{R}^N$$

Real Critical Points

- The integral in the spinfoam amplitude has the following form:

$$\int \mathrm{d}^N x \, \mu(x) \, e^{\lambda S(r,x)}, \quad \lambda \gg 1,$$

where r is boundary data, x is integration variable.

$$r = (j_b, \xi_{eb}), \quad x = \{j_h, x_{ve}, y_{ve}, x_{vf}, y_{vf}\} \in \mathbb{R}^N$$

- *Real critical point* $\mathring{x}$ is the solution of the critical equations

$$\mathrm{Re}(S(\mathring{x})) = \partial_x S(\mathring{x}) = 0,$$

Real Critical Points

- The integral in the spinfoam amplitude has the following form:

$$\int \mathrm{d}^N x \, \mu(x) \, e^{\lambda S(r,x)}, \quad \lambda \gg 1,$$

where r is boundary data, x is integration variable.

$$r = (j_b, \xi_{eb}), \quad x = \{j_h, x_{ve}, y_{ve}, x_{vf}, y_{vf}\} \in \mathbb{R}^N$$

- *Real critical point* $\mathring{x}$ is the solution of the critical equations

$$\mathrm{Re}(S(\mathring{x})) = \partial_x S(\mathring{x}) = 0,$$

- The solution gives Regge geometries subject to the flatness constraint (up to some "parity flips"):

$$\gamma \delta_h = 0 \mod 4\pi\mathbb{Z}.$$

- Spinfoam amplitudes seem to be dominated *only* by flat Regge geometries in the semiclassical regime.

Δ_3 triangulation

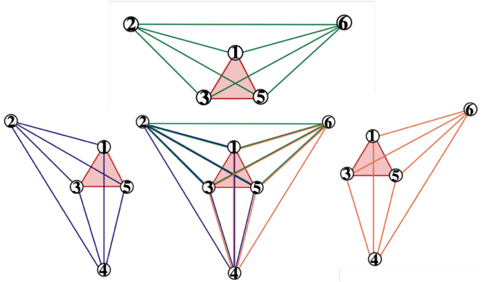

[Dona, Gozzini, Sarno, 2020]

- Δ_3 contains three 4-simplices and a single internal face h.
- All edges are on the boundary, boundary edge-lengths determine Regge geometry on Δ_3.
- $r = \{j_b, \xi_{eb}\}$ is the boundary data, determining boundary edge-lengths, and Regge geometry $\mathbf{g}(r)$.
- All tetrahedra and triangles are spacelike.

Flatness Problem

- Regime 1: fixing the boundary data r admits a flat geometry on the triangulation

$$\int \mathrm{d}^N x\, \mu(x)\, e^{\lambda S(r,x)} = \left(\frac{1}{\lambda}\right)^{\frac{N}{2}} \frac{e^{\lambda S(r,\mathring{x})}\mu(\mathring{x})}{\sqrt{\det\left(-\delta^2_{x,x} S(r,\mathring{x})/2\pi\right)}} \left[1 + O(1/\lambda)\right]. \tag{1}$$

The dominant contribution comes from the real critical point.

Flatness Problem

- Regime 1: fixing the boundary data r admits a flat geometry on the triangulation

$$\int \mathrm{d}^N x\, \mu(x)\, e^{\lambda S(r,x)} = \left(\frac{1}{\lambda}\right)^{\frac{N}{2}} \frac{e^{\lambda S(r,\mathring{x})}\mu(\mathring{x})}{\sqrt{\det\left(-\delta^2_{x,x} S(r,\mathring{x})/2\pi\right)}} \left[1 + O(1/\lambda)\right]. \tag{1}$$

  The dominant contribution comes from the real critical point.

- Regime 2: fixing the boundary data r only admits the curved geometry, no real critical point, the amplitude is suppressed:

$$\int \mathrm{d}^N x\, \mu(x)\, e^{\lambda S(r,x)} = O(\lambda^{-K}), \quad \forall\, K > 0. \tag{2}$$

Flatness Problem

- Regime 1: fixing the boundary data r admits a flat geometry on the triangulation

$$\int \mathrm{d}^N x \, \mu(x) \, e^{\lambda S(r,x)} = \left(\frac{1}{\lambda}\right)^{\frac{N}{2}} \frac{e^{\lambda S(r,\mathring{x})} \mu(\mathring{x})}{\sqrt{\det\left(-\delta^2_{x,x} S(r,\mathring{x})/2\pi\right)}} \left[1 + O(1/\lambda)\right]. \tag{1}$$

  The dominant contribution comes from the real critical point.

- Regime 2: fixing the boundary data r only admits the curved geometry, no real critical point, the amplitude is suppressed:

$$\int \mathrm{d}^N x \, \mu(x) \, e^{\lambda S(r,x)} = O(\lambda^{-K}), \quad \forall\, K > 0. \tag{2}$$

- We also let r vary, then we need an interpolation between two regimes (1) and (2) in order to clarify contributions from curved geometries $\longrightarrow$ the use of *complex critical point.*

Complex Critical Points

We consider the large-λ integral:

$$\int_K \mathrm{d}^N x \, \mu(x) \, e^{\lambda S(r,x)}, \quad N = 124 \text{ for } \Delta_3,$$

- $S(r,x)$ and $\mu(x)$ are analytic functions for $r \in U \subset \mathbb{R}^k, x \in K \subset \mathbb{R}^N$.
- $U \times K$ is a compact neighborhood of $(\mathring{r}, \mathring{x})$.

Analytic Extension

$$x \to z \in \mathbb{C}^N, \quad S(r,x) \to \mathcal{S}(r,z)$$

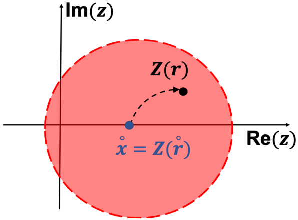

Complex critical points $z = Z(r)$ are the solutions of the complex critical equation

$$\partial_z \mathcal{S} = 0$$

Complex Critical Points

[Hörmander, 1983; Melin, Sjöstrand, 1975]

Large-λ asymptotic expansion for the integral

$$\int_K \mathrm{d}^N x\, \mu(x) e^{\lambda S(r,x)} = \left(\frac{1}{\lambda}\right)^{\frac{N}{2}} \frac{e^{\lambda \mathcal{S}(r,Z(r))}\mu(Z(r))}{\sqrt{\det\left(-\delta^2_{z,z}\mathcal{S}(r,Z(r))/2\pi\right)}}\left[1+O(1/\lambda)\right]$$

- The dominant contribution from the complex critical point.

Complex Critical Points

[Hörmander, 1983; Melin, Sjöstrand, 1975]

Large-λ asymptotic expansion for the integral

$$\int_K \mathrm{d}^N x\, \mu(x) e^{\lambda S(r,x)} = \left(\frac{1}{\lambda}\right)^{\frac{N}{2}} \frac{e^{\lambda \mathcal{S}(r,Z(r))}\mu(Z(r))}{\sqrt{\det\left(-\delta^2_{z,z}\mathcal{S}(r,Z(r))/2\pi\right)}}\left[1+O(1/\lambda)\right]$$

- The dominant contribution from the complex critical point.
- Interpolating two regimes:

$$\begin{cases} r = \mathring{r}, & \mathrm{Re}(\mathcal{S}(\mathring{r}, Z(\mathring{r})) = 0, \quad \text{power-law decay.} \\ r \neq \mathring{r}, & \mathrm{Re}(\mathcal{S}(r, Z(r)) < 0, \quad \text{damping factor } e^{\lambda \mathrm{Re}(\mathcal{S})} \end{cases}$$

Complex Critical Points

[Hörmander, 1983; Melin, Sjöstrand, 1975]

Large-λ asymptotic expansion for the integral

$$\int_K \mathrm{d}^N x\, \mu(x) e^{\lambda S(r,x)} = \left(\frac{1}{\lambda}\right)^{\frac{N}{2}} \frac{e^{\lambda \mathcal{S}(r,Z(r))}\mu(Z(r))}{\sqrt{\det\left(-\delta^2_{z,z}\mathcal{S}(r,Z(r))/2\pi\right)}}\,[1+O(1/\lambda)]$$

- The dominant contribution from the complex critical point.
- Interpolating two regimes:

$$\begin{cases} r = \mathring{r}, & \mathrm{Re}(\mathcal{S}(\mathring{r}, Z(\mathring{r})) = 0, & \text{power-law decay.} \\ r \neq \mathring{r}, & \mathrm{Re}(\mathcal{S}(r, Z(r)) < 0, & \text{damping factor } e^{\lambda \mathrm{Re}(\mathcal{S})} \end{cases}$$

- $\frac{1}{\lambda}$ is a *finite* expansion parameter, like $\hbar$ in quantum mechanics.

Complex Critical Points

[Hörmander, 1983; Melin, Sjöstrand, 1975]

Large-λ asymptotic expansion for the integral

$$\int_K \mathrm{d}^N x\, \mu(x) e^{\lambda S(r,x)} = \left(\frac{1}{\lambda}\right)^{\frac{N}{2}} \frac{e^{\lambda \mathcal{S}(r,Z(r))}\mu(Z(r))}{\sqrt{\det\left(-\delta^2_{z,z}\mathcal{S}(r,Z(r))/2\pi\right)}} \left[1 + O(1/\lambda)\right]$$

- The dominant contribution from the complex critical point.
- Interpolating two regimes:

$$\begin{cases} r = \mathring{r}, & \mathrm{Re}(\mathcal{S}(\mathring{r}, Z(\mathring{r})) = 0, & \text{power-law decay.} \\ r \neq \mathring{r}, & \mathrm{Re}(\mathcal{S}(r, Z(r)) < 0, & \text{damping factor } e^{\lambda \mathrm{Re}(\mathcal{S})} \end{cases}$$

- $\frac{1}{\lambda}$ is a *finite* expansion parameter, like $\hbar$ in quantum mechanics.
- Given any λ, $e^{\lambda \mathrm{Re}(\mathcal{S})}$ may not be small, e.g. $e^{\lambda \mathrm{Re}(\mathcal{S})} = e^{-1}$ if $\mathrm{Re}(\mathcal{S}) = -1/\lambda$.

Outline

Δ_3 triangulation

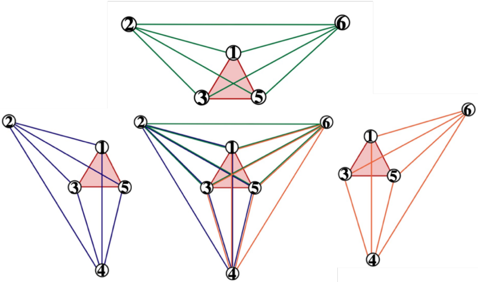

- Δ_3 contains three 4-simplices and a single internal face h.
- All edges are on the boundary, boundary edges-lengths determine Regge geometry on Δ_3.
- $r = \{j_b, \xi_{eb}\}$ is the boundary data, determining boundary edge-lengths, and Regge geometry $\mathbf{g}(r)$.
- All tetrahedra and triangles are spacelike.

[Dona, Gozzini, Sarno, 2020]

We numerically construct boundary data, flat geometry, and real critical point.

$\xi_{a,b}$ b / a	1	2	3	4	5
1	$\diagdown$	(1.,0.01 + 0.01i)	(0.87,0.01+0.49i)	(0.87,0.46+0.17i)	(0.3, -0.55-0.78i)
2	(1,-0.01,-0.01i)	$\diagdown$	(0.49,0.02+0.87i)	(0.49,0.82+0.31i)	(0.95,-0.17-0.25i)
3	(0.86,-0.01+0.51i)	(0.51,-0.02+0.86i)	$\diagdown$	(0.71,0.56-0.43i)	(0.71,-0.24+0.67i)
4	(0.86,0.48+0.16i)	(0.51,0.82+0.27i)	(0.71,0.59-0.39i)	$\diagdown$	**(0.71, 0.71)**
5	(0.3,-0.55-0.78i)	(0.95,-0.17-0.25i)	(0.71,-0.24+0.67i)	**(0.71, 0.71)**	$\diagdown$

a	1	2	3
$\mathring{g}_a$	$\begin{pmatrix} 1.16 & 0.06-0.09i \\ 0.06+0.09i & 0.87 \end{pmatrix}$	$\begin{pmatrix} 0.87 & 0.06-0.09i \\ 0.06+0.09i & 1.16 \end{pmatrix}$	$\begin{pmatrix} 1.02 & 0.06+0.17i \\ 0.06-0.17i & 1.02 \end{pmatrix}$
a	4	5	
$\mathring{g}_a$	$\begin{pmatrix} 1.03 & 0 \\ -0.36 & 0.97 \end{pmatrix}$	$\begin{pmatrix} 1 & 0 \\ 0 & 1 \end{pmatrix}$	

$\xi_{a,b}$ b / a	6	7	8	9	10
6	$\diagdown$	(0.95,-0.17-0.25i)	**(0.71, 0.71)**	(0.71,-0.24+0.67i)	(0.3,-0.55-0.78i)
7	(0.95,-0.17-0.25i)	$\diagdown$	(0.29,-0.47+0.83i)	(0.88,-0.02-0.48i)	(1,-0.02-0.03i)
8	**(0.71, 0.71)**	(0.31,-0.57+0.76i)	$\diagdown$	(0.71,0.25+0.66i)	(0.31,0.57-0.76i)
9	(0.71,-0.24+0.67i)	(0.85,0.02-0.52i)	(0.71,0.19+0.68i)	$\diagdown$	(0.85,-0.02+0.52i)
10	(0.3,-0.55-0.78i)	(1,0.02+0.03i)	(0.29,0.47-0.83i)	(0.88,0.02+0.48i)	$\diagdown$

a	6	7	8
$\mathring{g}_a$	$\begin{pmatrix} 1 & 0 \\ 0 & 1 \end{pmatrix}$	$\begin{pmatrix} 1.26 & -0.09+0.13i \\ -0.09-0.13i & 0.82 \end{pmatrix}$	$\begin{pmatrix} 0.97 & -0.34 \\ 0 & 1.03 \end{pmatrix}$
a	9	10	
$\mathring{g}_a$	$\begin{pmatrix} 1.04 & -0.09-0.25i \\ -0.09+0.25i & 1.04 \end{pmatrix}$	$\begin{pmatrix} 0.82 & -0.09+0.13i \\ -0.09-0.13i & 1.26 \end{pmatrix}$	

$\xi_{a,b}$ b / a	11	12	13	14	15
11	$\diagdown$	**(0.71, 0.71)**	(0.31,-0.57+0.76i)	(0.71,0.25+0.66i)	(0.31,0.57-0.76i)
12	**(0.71, 0.71)**	$\diagdown$	(0.51,0.82+0.27i)	(0.71,0.59-0.39i)	(0.86,0.48+0.16i)
13	(0.31,-0.57+0.76i)	(0.51,0.82+0.27i)	$\diagdown$	(0.5,0.87i)	(0,0.95+0.31i)
14	(0.71,0.25+0.66i)	(0.71,0.59-0.39i)	(0.5,0.87i)	$\diagdown$	(0.5,-0.87i)
15	(0.31,0.57-0.76i)	(0.86,0.48+0.16i)	(0,-0.95-0.31i)	(0.5,-0.87i)	$\diagdown$

a	11	12	13
$\mathring{g}_a$	$\begin{pmatrix} 1.04 & 0.02 \\ 0.36 & 0.97 \end{pmatrix}$	$\begin{pmatrix} 0.97 & 0.36 \\ 0 & 1.03 \end{pmatrix}$	$\begin{pmatrix} 1.02+0.0005i & 0.19-0.003i \\ 0.19+0.003i & 1.01-0.0005i \end{pmatrix}$
a	14	15	
$\mathring{g}_a$	$\begin{pmatrix} 1.02-0.001i & 0.19+0.006i \\ 0.19-0.006i & 1.02+0.001i \end{pmatrix}$	$\begin{pmatrix} 1.02+0.0005i & 0.19-0.003i \\ 0.19+0.003i & 1.01-0.0005i \end{pmatrix}$	

area $j_{a,b}$ b / b	2	3	4	5
1	2	2	2	5
2	$\diagdown$	2	2	5
3	$\diagdown$	$\diagdown$	2	5
4	$\diagdown$	$\diagdown$	$\diagdown$	**5**

area $j_{a,b}$ b / b	7	8	9	10
6	5	**5**	5	5
7	$\diagdown$	4.71	5.19	5.19
8	$\diagdown$	$\diagdown$	4.71	4.71
9	$\diagdown$	$\diagdown$	$\diagdown$	5.19

area $j_{a,b}$ b / a	12	13	14	15
11	**5**	4.71	4.71	4.71
12	$\diagdown$	2	2	2
13	$\diagdown$	$\diagdown$	3.18	3.18
14	$\diagdown$	$\diagdown$	$\diagdown$	3.18

$\vert\mathring{z}_{a,b}\rangle$ b / a	2	3	4	5
1	(1,0.06 + 0.08i)	(1,0.07 + 0.47i)	(1,0.42 + 0.22i)	(1,-1.82 - 2.57i)
2	$\diagdown$	(1,0.31 + 2.08i)	(1,1.86 + 0.99i)	(1,-0.18 - 0.26i)
3	$\diagdown$	$\diagdown$	(1,0.68 - 0.73i)	(1,-0.33 + 0.94i)
4	$\diagdown$	$\diagdown$	$\diagdown$	(1,1)

Algorithm of $A(\Delta_3)$

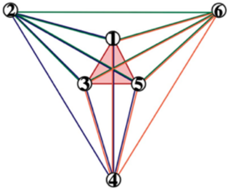

- We vary the length l_{26}. It gives a family of boundary data $r = \mathring{r} + \delta r$. We obtain numerically a family of curved geometries $\mathbf{g}(r)$:

$$\begin{aligned} \text{Length variation } \delta l_{26} : &\quad 0.7 \times 10^{-12} \sim 10^{-4} \\ \text{Deficit angle } \delta_h : &\quad 1.4 \times 10^{-12} \sim 0.0002 \end{aligned}$$

- For each $\delta_h \neq 0$, the real critical point is absent.
- Numerically compute the complex critical point $z = Z(r)$ satisfying $\partial_z \mathcal{S}(r, z) = 0$ with Newton-like recursive procedure:

Algorithm of $A(\Delta_3)$

1. We linearize $\partial_z \mathcal{S}(r,z) = 0$ at $x_0 \in \mathbb{R}^{124}$ (satisfying $\mathrm{Re}(S) = \partial_g S = \partial_{\mathbf{z}} S = 0$, but $\partial_{j_h} S \neq 0$)

$$\partial_z \mathcal{S}(r, x_0) + \partial_z^2 \mathcal{S}(r, x_0) \cdot \delta z_1 = 0,$$

   the solution is $z_1 = x_0 + \delta z_1$.

2. Similarly, we linearize $\partial_z \mathcal{S}(r,z) = 0$ at z_1, the solution is $z_2 = z_1 + \delta z_2$.
3. We linearize $\partial_z \mathcal{S}(r,z) = 0$ at z_2, $\cdots\cdots$
4. $\cdots\cdots$
5. We linearize $\partial_z \mathcal{S}(r,z) = 0$ at z_{n-1}, the solution approximates the complex critical point $Z(r) \simeq z_n = z_{n-1} + \delta z_n$.
6. Practically, we use $n = 4$.
7. Absolute Error: $\varepsilon = \max |\partial_z \mathcal{S}(r, z_n)| \approx 1.31 \delta_h^5$.

δ_h	2×10^{-16}	2×10^{-12}	3×10^{-8}	6×10^{-6}	4×10^{-5}	2×10^{-4}
ε	2×10^{-79}	4.27×10^{-59}	3.19×10^{-38}	1.02×10^{-26}	1.34×10^{-22}	4.2×10^{-19}

Numerical Results

We numerically compute the complex critical point $Z(r)$ for many r corresponding to curved geometries.

We compute numerically $\mathcal{S}$ and the difference $\delta\mathcal{I}(r)$ from the Regge action of the curved geometry $\mathbf{g}(r)$:

$$\mathcal{S}(r, Z(r)) = i\mathcal{I}_R[\mathbf{g}(r)] + \delta\mathcal{I}(r), \quad \mathcal{I}_R[\mathbf{g}(r)] = \mathfrak{a}_h(r)\delta_h(r) + \sum_b \mathfrak{a}_b(r)\Theta_b(r).$$

At $\lambda = 10^{11}, \gamma = 0.1$,

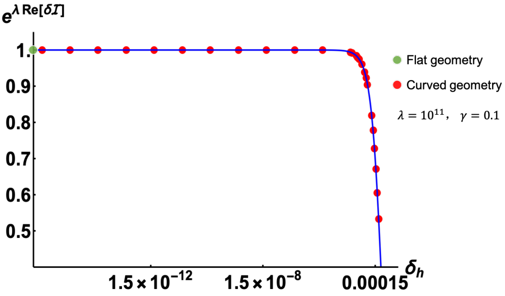

Numerical Results

We numerically fit $e^{\lambda \mathrm{Re}(\delta \mathcal{I})}$ (blue curve) and $e^{i\lambda \mathrm{Im}(\delta \mathcal{I})}$

$$\delta \mathcal{I} = a_2 \delta_h^2 + a_3 \delta_h^3 + a_4 \delta_h^4 + O(\delta_h^5)$$

The best fit coefficient a_i and the corresponding fitting errors at $\gamma = 0.1$ are

$$\begin{aligned} a_2 &= -0.00016_{\pm 10^{-17}} - i0.00083_{\pm 10^{-16}}, \\ a_3 &= -0.0071_{\pm 10^{-13}} - i0.011_{\pm 10^{-12}}, \\ a_4 &= -0.059_{\pm 10^{-9}} + i0.070_{\pm 10^{-8}}. \end{aligned}$$

The effective action $\mathcal{S}$ is the Regge action plus "high curvature correction":

$$\mathcal{S}(r, Z(r)) = i\mathcal{I}_R[\mathbf{g}(r)] + \delta \mathcal{I}(r),$$

Large-λ asymptotic expansion for the integral

$$\int_K \mathrm{d}^N x\, \mu(x) e^{\lambda S(r,x)} = \left(\frac{1}{\lambda}\right)^{\frac{N}{2}} \frac{e^{\lambda \mathcal{S}(r,Z(r))} \mu(Z(r))}{\sqrt{\det\left(-\delta^2_{z,z} \mathcal{S}(r, Z(r))/2\pi\right)}} [1 + O(1/\lambda)]$$

Numerical Results

The contour plots of $e^{\lambda \mathrm{Re}[\delta \mathcal{I}(r)]} \propto |A(\Delta_3)|$:

$\gamma = 0.1$ $\lambda = 5 \times 10^{10}$

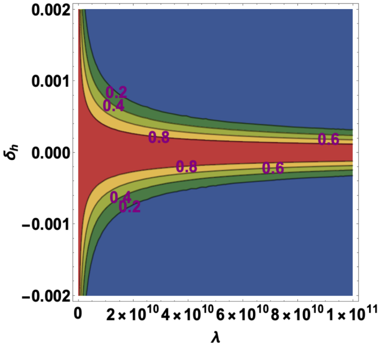

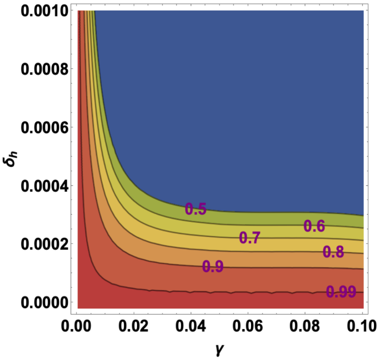

The non-blue regime of curved geometries where $A(\Delta_3)$ is not small.

Cosine Problem

Natively,

$$\begin{aligned} A(\Delta_3) &\sim (e^{i\mathcal{I}_R}+e^{-i\mathcal{I}_R})(e^{i\mathcal{I}_R}+e^{-i\mathcal{I}_R})(e^{i\mathcal{I}_R}+e^{-i\mathcal{I}_R}) \\ &= 8 \text{ terms} \end{aligned}$$

- 8 terms correspond to 2 continuous 4-simplex orientations

  $$+++,\ ---$$

  and 6 discontinuous 4-simplex orientations:

  $$++-,\ +--,\ --+,\ -+-,\ +-+,\ -++,$$

Cosine Problem

- Flatness constraint changes to:

$$\gamma\delta_h^s = \gamma \sum_{v\in h} s_v \Theta_h(v) = 0 \mod 4\pi\mathbb{Z},$$

$s_v = \pm$ are opposite orientations at the 4-simplex v.

- Given the boundary data $\mathring{r}$,

s	$+++$	$---$	$++-$	$--+$	$+--$	$-++$	$-+-$	$+-+$
δ_h^s	0	0	0.043	-0.043	0.72	-0.72	-0.68	0.68

there are only 2 real critical points with all $s_v = +$ or $s_v = -$.

Asymptotics of $A(\Delta_3)$

- With $r = \mathring{r} + \delta r$ of curved geometries $\mathbf{g}(r)$

$$A(\Delta_3) \sim \left(\frac{1}{\lambda}\right)^{62} \left[\mathscr{N}_+ e^{i\lambda \mathcal{I}_R[\mathbf{g}(r)] + \lambda \delta \mathcal{I}(r)} + \mathscr{N}_- e^{-i\lambda \mathcal{I}_R[\mathbf{g}(r)] + \lambda \delta \mathcal{I}'(r)}\right]$$

contributed by the complex critical points close to these 2 real critical points.

Cosine problem is relaxed in this example.

$$\begin{aligned}
\text{Regge action: } \mathcal{I}_R &= \mathfrak{a}_h \delta_h + \sum_b \mathfrak{a}_b \Theta_b, \\
\text{High curvature correction: } \delta\mathcal{I} &= a_2 \delta_h^2 + a_3 \delta_h^3 + a_4 \delta_h^4 + O(\delta_h^5), \\
\delta\mathcal{I}' &= \bar{a}_2 \delta_h^2 - \bar{a}_3 \delta_h^3 + \bar{a}_4 \delta_h^4 + O(\delta_h^5)
\end{aligned}$$

Outline

1-5 Pachner move

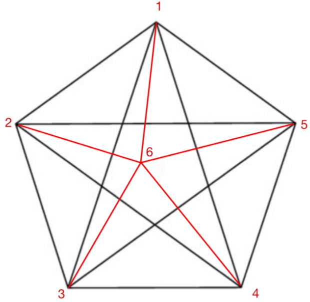

- σ_{1-5}: the complex of the 1-5 Pachner move refining a 4-simplex into five 4-simplices.
- Simplicial complex: 1 internal site, 5 internal segments (red), 10 boundary triangles b, and 10 internal triangles h.

$$
\begin{aligned}
A(\sigma_{1\text{-}5}) &= \int \mathrm{d}j_{12}\mathrm{d}j_{13}\mathrm{d}j_{14}\mathrm{d}j_{15}\mathrm{d}j_{23}\, \mathcal{Z}_{\sigma_{1\text{-}5}}\left(j_{12}, j_{13}, j_{14}, j_{15}, j_{23}\right), \\
\mathcal{Z}_{\sigma_{1\text{-}5}} &= \sum_{\{k_h\}} \int \prod_{\bar{h}=1}^{5} \mathrm{d}j_{\bar{h}} \prod_{h=1}^{10} (2\lambda) d_{\lambda j_h} \int [\mathrm{d}g\mathrm{d}\mathbf{z}] e^{\lambda S^{(k)}},
\end{aligned}
$$

1-5 Pachner move

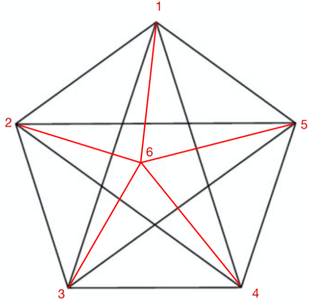

- σ_{1-5}: the complex of the 1-5 Pachner move refining a 4-simplex into five 4-simplices.
- Simplicial complex: 1 internal site, 5 internal segments (red), 10 boundary triangles b, and 10 internal triangles h.
- Regge geometries $\mathbf{g}(r)$ are determined by the boundary data and five lengths $l_{m6}, m = 1, 2, 3, 4, 5$.
- Locally change variables (Heron's formula): $l_{m6} \to j_{12}, j_{13}, j_{14}, j_{15}, j_{23}$.

$$
\begin{aligned}
A(\sigma_{1\text{-}5}) &= \int \mathrm{d}j_{12}\mathrm{d}j_{13}\mathrm{d}j_{14}\mathrm{d}j_{15}\mathrm{d}j_{23}\, \mathcal{Z}_{\sigma_{1\text{-}5}}\left(j_{12}, j_{13}, j_{14}, j_{15}, j_{23}\right), \\
\mathcal{Z}_{\sigma_{1\text{-}5}} &= \sum_{\{k_h\}} \int \prod_{\bar{h}=1}^{5} \mathrm{d}j_{\bar{h}} \prod_{h=1}^{10} (2\lambda) d_{\lambda j_h} \int [\mathrm{d}g\mathrm{d}\mathbf{z}] e^{\lambda S^{(k)}},
\end{aligned}
$$

1-5 Pachner move

$$A(\sigma_{1\text{-}5}) = \int \mathrm{d}j_{12}\mathrm{d}j_{13}\mathrm{d}j_{14}\mathrm{d}j_{15}\mathrm{d}j_{23}\, \mathcal{Z}_{\sigma_{1\text{-}5}}(j_{12}, j_{13}, j_{14}, j_{15}, j_{23})$$

$$\mathcal{Z}_{\sigma_{1\text{-}5}} = \sum_{\{k_h\}} \int \prod_{\bar{h}=1}^{5} \mathrm{d}j_{\bar{h}} \prod_{h=1}^{10} (2\lambda) d_{\lambda j_h} \int [\mathrm{d}g\mathrm{d}\mathbf{z}] e^{\lambda S^{(k)}},$$

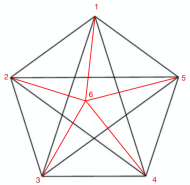

- We focus on the 195-dim integral in $\mathcal{Z}_{\sigma_{1\text{-}5}}$ with $k_h = 0$.

1-5 Pachner move

$$
\begin{aligned}
A(\sigma_{1\text{-}5}) &= \int \mathrm{d}j_{12}\mathrm{d}j_{13}\mathrm{d}j_{14}\mathrm{d}j_{15}\mathrm{d}j_{23}\, \mathcal{Z}_{\sigma_{1\text{-}5}}(j_{12}, j_{13}, j_{14}, j_{15}, j_{23}) \\
\mathcal{Z}_{\sigma_{1\text{-}5}} &= \sum_{\{k_h\}} \int \prod_{\bar{h}=1}^{5} \mathrm{d}j_{\bar{h}} \prod_{h=1}^{10} (2\lambda) d_{\lambda j_h} \int [\mathrm{d}g\mathrm{d}\mathbf{z}] e^{\lambda S^{(k)}},
\end{aligned}
$$

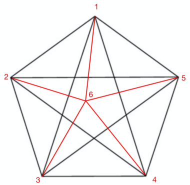

- We focus on the 195-dim integral in $\mathcal{Z}_{\sigma_{1\text{-}5}}$ with $k_h = 0$.
- For $\mathcal{Z}_{\sigma_{1\text{-}5}}$, the external parameters: $r = \{j_{12}, j_{13}, j_{14}, j_{15}, j_{23}; j_b, \xi_{eb}\}$. $\mathring{r}$ determines the flat geometry $\mathbf{g}(\mathring{r})$, and the real critical point $\{\mathring{j}_{\bar{h}}, \mathring{g}_{ve}, \mathring{\mathbf{z}}_{vf}\}$ with all $s_v = +$.

1-5 Pachner move

$$
\begin{aligned}
A(\sigma_{1\text{-}5}) &= \int \mathrm{d}j_{12}\mathrm{d}j_{13}\mathrm{d}j_{14}\mathrm{d}j_{15}\mathrm{d}j_{23}\, \mathcal{Z}_{\sigma_{1\text{-}5}}\,(j_{12}, j_{13}, j_{14}, j_{15}, j_{23}) \\
\mathcal{Z}_{\sigma_{1\text{-}5}} &= \sum_{\{k_h\}} \int \prod_{\bar{h}=1}^{5} \mathrm{d}j_{\bar{h}} \prod_{h=1}^{10} (2\lambda) d_{\lambda j_h} \int [\mathrm{d}g\mathrm{d}\mathbf{z}] e^{\lambda S^{(k)}},
\end{aligned}
$$

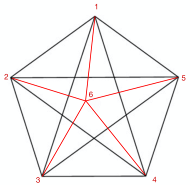

- We focus on the 195-dim integral in $\mathcal{Z}_{\sigma_{1\text{-}5}}$ with $k_h = 0$.
- For $\mathcal{Z}_{\sigma_{1\text{-}5}}$, the external parameters: $r = \{j_{12}, j_{13}, j_{14}, j_{15}, j_{23}; j_b, \xi_{eb}\}$. $\mathring{r}$ determines the flat geometry $\mathbf{g}(\mathring{r})$, and the real critical point $\{\mathring{j}_{\bar{h}}, \mathring{g}_{ve}, \mathring{\mathbf{z}}_{vf}\}$ with all $s_v = +$.
- Fixing $\mathring{j}_b, \mathring{\xi}_{eb}$, we deform $l_{m6} = \mathring{l}_{m6} + \delta l_{m6}$, so that e.g. $j_{12} = \mathring{j}_{12} + \delta j_{12}, \cdots$, and $r = \mathring{r} + \delta r$, using Monte-Carlo method.

1-5 Pachner move

$$A(\sigma_{1\text{-}5}) = \int \mathrm{d}j_{12}\mathrm{d}j_{13}\mathrm{d}j_{14}\mathrm{d}j_{15}\mathrm{d}j_{23}\, \mathcal{Z}_{\sigma_{1\text{-}5}}(j_{12}, j_{13}, j_{14}, j_{15}, j_{23})$$

$$\mathcal{Z}_{\sigma_{1\text{-}5}} = \sum_{\{k_h\}} \int \prod_{\bar{h}=1}^{5} \mathrm{d}j_{\bar{h}} \prod_{h=1}^{10} (2\lambda) d_{\lambda j_h} \int [\mathrm{d}g\mathrm{d}\mathbf{z}] e^{\lambda S^{(k)}},$$

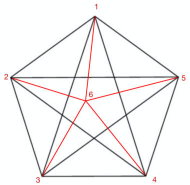

- We focus on the 195-dim integral in $\mathcal{Z}_{\sigma_{1\text{-}5}}$ with $k_h = 0$.
- For $\mathcal{Z}_{\sigma_{1\text{-}5}}$, the external parameters: $r = \{j_{12}, j_{13}, j_{14}, j_{15}, j_{23}; j_b, \xi_{eb}\}$. $\mathring{r}$ determines the flat geometry $\mathbf{g}(\mathring{r})$, and the real critical point $\{\mathring{j}_{\bar{h}}, \mathring{g}_{ve}, \mathring{\mathbf{z}}_{vf}\}$ with all $s_v = +$.
- Fixing $\mathring{j}_b, \mathring{\xi}_{eb}$, we deform $l_{m6} = \mathring{l}_{m6} + \delta l_{m6}$, so that e.g. $j_{12} = \mathring{j}_{12} + \delta j_{12}, \cdots$, and $r = \mathring{r} + \delta r$, using Monte-Carlo method.
- There are 4 DoFs of deformation δr keeping the geometry flat.
- There is 1 DoF $r = \mathring{r} + \delta r$. $\mathbf{g}(r)$ are curved geometries with small deficit angles $< 10^{-3}$. The real critical point is absent.

- Compute numerically complex critical points $Z(r)$ for many r.
- $\mathcal{S}(r, Z(r)) = i\mathcal{I}_R[\mathbf{g}(r)] + \delta\mathcal{I}(r)$,

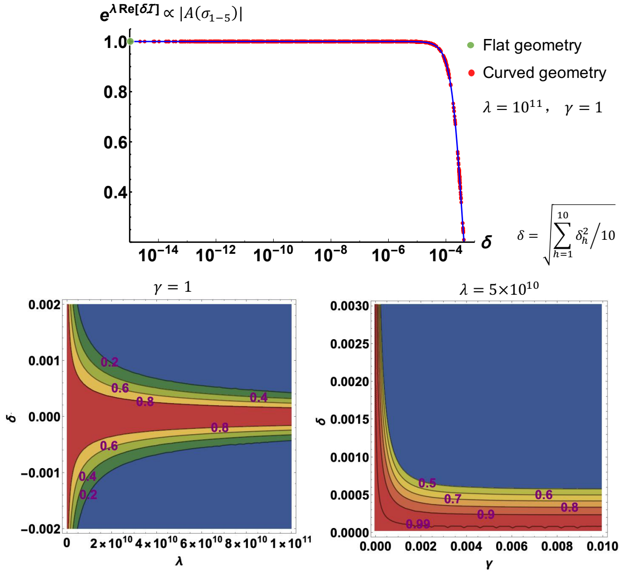

1-5 Pachner move

$$A(\sigma_{1\text{-}5}) \quad = \quad \int \mathrm{d}j_{12}\mathrm{d}j_{13}\mathrm{d}j_{14}\mathrm{d}j_{15}\mathrm{d}j_{23}\, \mathcal{Z}_{\sigma_{1\text{-}5}}\left(j_{12}, j_{13}, j_{14}, j_{15}, j_{23}\right),$$

Insert the asymptotic expansion of $\mathcal{Z}_{\sigma_{1\text{-}5}}$ back in $A(\sigma_{1\text{-}5})$, we obtain integral over Regge geometries:

$$\left(\frac{1}{\lambda}\right)^{\frac{N}{2}} \int \prod_{m=1}^{5} \mathrm{d}l_{m6}\, e^{\lambda \mathcal{S}(r, Z(r))} \mathscr{N}_r \left[1 + O(1/\lambda)\right],$$

we have changed $\mathrm{d}j \to \mathrm{d}l$ and $r = r(l)$.

The action is Regge action plus “high curvature correction”:

$$\mathcal{S}(r, Z(r)) = i\mathcal{I}_R[\mathbf{g}(r)] - a(\gamma)\delta(r)^2 + O(\delta^3),$$

$\gamma = 1$, $a = 8.88 \times 10^{-5}_{\pm 10^{-12}} - i0.033_{\pm 10^{-10}}$.

Summary

- EPRL spinfoam amplitudes allow curved Regge geometries with small deficit angles.

Summary

- EPRL spinfoam amplitudes allow curved Regge geometries with small deficit angles.
- The curved geometries correspond to complex critical points that are slightly away from the real integration domain.

Summary

- EPRL spinfoam amplitudes allow curved Regge geometries with small deficit angles.
- The curved geometries correspond to complex critical points that are slightly away from the real integration domain.
- Regge geometries with small deficit angles are sufficient for approximating arbitrary smooth curved geometry.

Summary

- EPRL spinfoam amplitudes allow curved Regge geometries with small deficit angles.
- The curved geometries correspond to complex critical points that are slightly away from the real integration domain.
- Regge geometries with small deficit angles are sufficient for approximating arbitrary smooth curved geometry.
- The dominant contribution to the spinfoam amplitude is proportional to $e^{\mathcal{S}}$, $\mathcal{S}$ is the Regge action of the curved geometry plus the curvature correction of order δ_h^2 and higher.

$$\mathcal{S} = i\mathcal{I}_R[\mathbf{g}(r)] + a_2\delta_h^2 + a_3\delta_h^3 + a_4\delta_h^4 + O(\delta_h^5),$$

Summary

- EPRL spinfoam amplitudes allow curved Regge geometries with small deficit angles.
- The curved geometries correspond to complex critical points that are slightly away from the real integration domain.
- Regge geometries with small deficit angles are sufficient for approximating arbitrary smooth curved geometry.
- The dominant contribution to the spinfoam amplitude is proportional to $e^{\mathcal{S}}$, $\mathcal{S}$ is the Regge action of the curved geometry plus the curvature correction of order δ_h^2 and higher.

$$\mathcal{S} = i\mathcal{I}_R[\mathbf{g}(r)] + a_2\delta_h^2 + a_3\delta_h^3 + a_4\delta_h^4 + O(\delta_h^5),$$

- Δ_3: relaxing cosine problem.

Summary

- EPRL spinfoam amplitudes allow curved Regge geometries with small deficit angles.
- The curved geometries correspond to complex critical points that are slightly away from the real integration domain.
- Regge geometries with small deficit angles are sufficient for approximating arbitrary smooth curved geometry.
- The dominant contribution to the spinfoam amplitude is proportional to $e^{\mathcal{S}}$, $\mathcal{S}$ is the Regge action of the curved geometry plus the curvature correction of order δ_h^2 and higher.

$$\mathcal{S} = i\mathcal{I}_R[\mathbf{g}(r)] + a_2\delta_h^2 + a_3\delta_h^3 + a_4\delta_h^4 + O(\delta_h^5),$$

- Δ_3: relaxing cosine problem.
- 1-5 Pachner move: reduce the spinfoam amplitude to integral over Regge geometries:

$$\left(\frac{1}{\lambda}\right)^{\frac{N}{2}} \int \prod_{m=1}^{5} \mathrm{d}l_{m6}\, e^{\lambda\mathcal{S}(r,Z(r))} \mathcal{N}_r \left[1 + O(1/\lambda)\right].$$

Outlook

- Other spinfoam models.
- Observables, e.g., correlation functions.
- More complicated complex.
- Lattice Refinement.
- Classical limit.
- Larger deficit angles and higher order correction.
- ...

Thank You!

Poisson summation

The spinfoam amplitude in the integral representation:

$$
\begin{aligned}
A(\mathcal{K}) &= \sum_{\{j_h\}}^{j^{\max}} \prod_h d_{j_h} \int [\mathrm{d}g\mathrm{d}\mathbf{z}]\, e^{S\left(j_h, g_{ve}, \mathbf{z}_{vf}; j_b, \xi_{eb}\right)}, \\
& \quad [\mathrm{d}g\mathrm{d}\mathbf{z}] = \prod_{(v,e)} \mathrm{d}g_{ve} \prod_{(v,f)} \mathrm{d}\Omega_{\mathbf{z}_{vf}},
\end{aligned}
$$

Without changing $A(\mathcal{K})$, we insert $\tau_{[-\epsilon, j^{\max}+\epsilon]}(j_h)$ with $0 < \epsilon < 1/2$ satisfying:

$$
\begin{aligned}
\tau_{[-\epsilon, j^{\max}+\epsilon]}(j_h) &= d_{j_h}, \quad j_h \in [0, j^{\max}], \\
\tau_{[-\epsilon, j^{\max}+\epsilon]}(j_h) &= 0, \quad j \notin [-\epsilon, j^{\max} + \epsilon]
\end{aligned}
$$

We apply the Poisson summation formula $\sum_{n\in\mathbb{Z}} f(n) = \sum_{k\in\mathbb{Z}} \int_{\mathbb{R}} \mathrm{d}n f(n)\, e^{2\pi i k n}$ to the sum over j_h:

$$
\begin{aligned}
A(\mathcal{K}) &= \sum_{\{k_h \in \mathbb{Z}\}} \int_{\mathbb{R}} \prod_h \mathrm{d}j_h \prod_h 2\tau_{[-\epsilon, j^{\max}+\epsilon]}(j_h) \int [\mathrm{d}g\mathrm{d}\mathbf{z}]\, e^{S^{(k)}}, \\
S^{(k)} &= S + 4\pi i \sum_h j_h k_h .
\end{aligned}
$$

Boundary Geometry

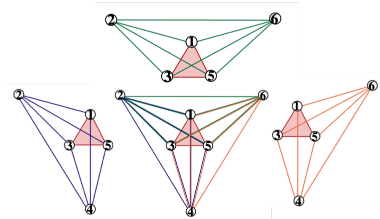

- Each 4-simplex is Lorentzian 4-simplex.
- All triangles and tetrahedra are space-like.

The length symmetry

$$
\begin{gathered}
l_{12} = l_{13} = l_{15} = l_{23} = l_{25} = l_{35} \approx 3.40, \\
l_{14} = l_{24} = l_{34} = l_{45} \approx 2.07, \\
l_{26} \approx 5.44, l_{46} \approx 3.24
\end{gathered}
$$

The coordinates for vertices:

$$
\begin{gathered}
P_1 = (0,0,0,0), P_2 = \left(0,0,0,-2\sqrt{5}/3^{1/4}\right), \\
P_3 = \left(0,0,-3^{1/4}\sqrt{5},-3^{1/4}\sqrt{5}\right) \\
P_4 = \left(0,-2\sqrt{10}/3^{3/4},-\sqrt{5}/3^{3/4},-\sqrt{5}/3^{1/4}\right), \\
P_5 = \left(-3^{-1/4}10^{-1/2},-\sqrt{5/2}/3^{3/4},-\sqrt{5}/3^{3/4},-\sqrt{5}/3^{1/4}\right), \\
P_6 = (0.90, 2.74, -0.98, -1.70).
\end{gathered}
$$

δ_h^s graph

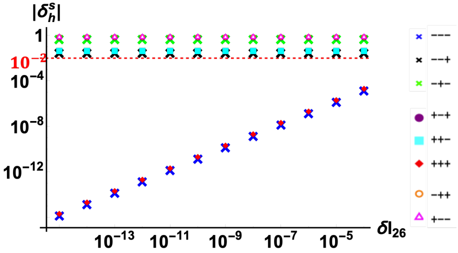

Numerical data for Pachner move

a	1	2	3
$\mathring{g}_a$	$\begin{pmatrix} 1.02 & -0.06-0.17i \\ -0.06+0.17i & 1.02 \end{pmatrix}$	$\begin{pmatrix} 0.99 & -0.06-0.17i \\ 0 & 1.01 \end{pmatrix}$	$\begin{pmatrix} 0.83 & -0.12-0.61i \\ 0 & 1.20 \end{pmatrix}$
a	4	5	
$\mathring{g}_a$	$\begin{pmatrix} 0.99 & 0.55+0.29i \\ 0.25 & 1.14+0.074i \end{pmatrix}$	$\begin{pmatrix} 0.94 & -0.12-0.45i \\ 0 & 1.02 \end{pmatrix}$	

$\lvert\mathring{z}_{a,b}\rangle$ b / a	2	3	4	5
1	(1,-0.33 + 0.94 i)	(1,0.08 - 0.69 i)	(0.68 - 0.73i)	(1,0.18 - 1.43 i)
2	$\diagdown$	(1,-0.14 + 1.50 i)	(1,-0.93 + 0.37i)	(1,-0.16 + 0.77i)
3	$\diagdown$	$\diagdown$	(1,-0.93 + 0.48i)	(1,0.078 - 0.58 i)
4	$\diagdown$	$\diagdown$	$\diagdown$	(1,0.64 - 0.88i)

a	6	7	8
$\mathring{g}_a$	$\begin{pmatrix} 1 & 0 \\ 0 & 1 \end{pmatrix}$	$\begin{pmatrix} 0.99 & -0.06-0.17i \\ 0 & 1.01 \end{pmatrix}$	$\begin{pmatrix} 1.03 & -0.03+0.045i \\ 0 & 0.96 \end{pmatrix}$
a	9	10	
$\mathring{g}_a$	$\begin{pmatrix} 0.98 & 0.25 \\ 0 & 1.02 \end{pmatrix}$	$\begin{pmatrix} 0.98 & -0.02+0.02i \\ 0 & 1.02 \end{pmatrix}$	

$\lvert\mathring{z}_{a,b}\rangle$ b / a	6	7	8	9	10
6	$\diagdown$	$\diagdown$	(1,1.82 + 2.57i)	(1,-1)	(0.18 + 0.26i)
7	(1,-0.33 + 0.94i)	$\diagdown$	$\diagdown$	$\diagdown$	$\diagdown$
8	$\diagdown$	(1,-0.14+ 1.50i)	$\diagdown$	(1,1.36 + 0.27i)	(1,4.60 + 6.50i)
9	$\diagdown$	(1,-0.93 + 0.37i)	$\diagdown$	$\diagdown$	(1,-1.11 - 0.072i)
10	$\diagdown$	(1,-0.16 + 0.77i)	$\diagdown$	$\diagdown$	$\diagdown$

a	11	12	13
$\mathring{g}_a$	$\begin{pmatrix} 1.08 & -0.03+0.04i \\ -0.03-0.04i & 0.93 \end{pmatrix}$	$\begin{pmatrix} 0.77 & -0.08-0.62i \\ 0.02+0.04i & 1.32-0.02i \end{pmatrix}$	$\begin{pmatrix} 0.96 & 0 \\ 0.03+0.04i & 1.04 \end{pmatrix}$
a	14	15	
$\mathring{g}_a$	$\begin{pmatrix} 0.85 & 0.45-0.11i \\ 0 & 1.18 \end{pmatrix}$	$\begin{pmatrix} 1.52 & -0.14+0.2i \\ 0 & 0.66 \end{pmatrix}$	

$\lvert\mathring{z}_{a,b}\rangle$ b / a	11	12	13	14	15
11	$\diagdown$	$\diagdown$	$\diagdown$	(1,1.77 + 0.80i)	(1,9.6 + 13.58i)
12	(1,0.03 - 0.62i)	$\diagdown$	(1,-0.23 + 1.31i)	$\diagdown$	$\diagdown$
13	(1,1.82 + 2.57i)	$\diagdown$	$\diagdown$	$\diagdown$	$\diagdown$
14	$\diagdown$	(1,-0.84 + 0.33i)	(1,1.21 + 0.14i)	$\diagdown$	(1,5.92 + 4.04i)
15	$\diagdown$	(1,0.027 - 0.53i)	(1,6.48 + 9.17i)	$\diagdown$	$\diagdown$

a	16	17	18
$\mathring{g}_a$	$\begin{pmatrix} 1.00 & -0.07 \\ -0.07 & 1.00 \end{pmatrix}$	$\begin{pmatrix} 0.96 & 0.27+0.28i \\ 0 & 1.04 \end{pmatrix}$	$\begin{pmatrix} 1.02 & 0 \\ -0.26 & 0.98 \end{pmatrix}$
a	19	20	
$\mathring{g}_a$	$\begin{pmatrix} 0.96+0.01i & 0.19-0.06i \\ -0.26-0.38i & 0.99 \end{pmatrix}$	$\begin{pmatrix} 1.01 & -0.12-0.01i \\ 0 & 0.99 \end{pmatrix}$	

$\lvert\mathring{z}_{a,b}\rangle$ b / a	16	17	18	19	20
16	$\diagdown$	$\diagdown$	$\diagdown$	$\diagdown$	(1,-1.7 - 0.68i)
17	(1,0.87 - 0.48i)	$\diagdown$	(1,-0.82 + 0.58i)	(1,-0.76 + 0.75i)	$\diagdown$
18	(1,-1)	$\diagdown$	$\diagdown$	(1,1.21 + 0.14i)	$\diagdown$
19	(1,1.51 + 0.42i)	$\diagdown$	$\diagdown$	$\diagdown$	$\diagdown$
20	$\diagdown$	(1,0.88 - 0.59i)	(1,-1.20 - 0.13i)	(1,2.54 + 0.65i)	$\diagdown$

a	21	22	23
$\mathring{g}_a$	$\begin{pmatrix} 0.87 & -0.06+0.086i \\ -0.06-0.085i & 1.16 \end{pmatrix}$	$\begin{pmatrix} 0.97 & -0.13-0.45i \\ 0 & 1.03 \end{pmatrix}$	$\begin{pmatrix} 0.98 & -0.016+0.023i \\ 0 & 1.02 \end{pmatrix}$
a	24	25	
$\mathring{g}_a$	$\begin{pmatrix} 1.64 & -0.17+0.24i \\ -0.05-0.07i & 0.62 \end{pmatrix}$	$\begin{pmatrix} 1.04 & -0.14-0.01i \\ 0.26 & 0.99-0.003i \end{pmatrix}$	

$\lvert\mathring{z}_{a,b}\rangle$ b / a	21	22	23	24	25
22	(1,0.18 - 1.43i)	$\diagdown$	(1,-0.15 + 0.78i)	(1,0.078 - 0.58i)	(1,0.64 - 0.88i)
23	(1,0.18 + 0.26i)	$\diagdown$	$\diagdown$	(1,4.6 + 6.5i)	(1,-1.11 - 0.072i)
24	(1,5.72 + 8.08i)	$\diagdown$	$\diagdown$	$\diagdown$	(1,4.58 + 3.90i)
25	(1,-1.41 - 0.31i)	$\diagdown$	$\diagdown$	$\diagdown$	$\diagdown$